Available online at www.sciencedirect.com
ScienceDirect
Thermochimica Acta 464 (2007) 29–34
thermochimica acta
www.elsevier.com/locate/tca

DSC approach for the investigation of mobile water fractions in aqueous solutions of NaCl and Tris buffer

P. Kamasa [a,*], M. Bokor [a], M. Pyda [b,c], K. Tompa [a]

[a] *Research Institute for Solid State Physics and Optics of Hungarian Academy of Sciences, POB 49, 1525 Budapest, Hungary*
[b] *Department of Chemistry, The University of Tennessee, Knoxville, TN 37996-1600, USA*
[c] *Department of Chemistry, The University of Technology, 35 959 Rzeszów, Poland*

Received 9 March 2007; received in revised form 3 August 2007; accepted 8 August 2007
Available online 15 August 2007

Abstract

The fraction of mobile (unfrozen) water during phase transitions of NaCl–H_2O solution and tris(hydroxymethyl)aminomethane (Tris) buffer solution has been determined by differential scanning calorimetry (DSC). Measurements were carried out in the temperature range between −50 and +30 °C with a heating rate of 2 K min^{-1}. The fraction of mobile water was estimated from the enthalpy of melting of the different frozen phases present in aqueous solution samples. Results are supplemented by proton NMR intensity measurements in the same temperature range. A small endothermic peak was detected in the DSC curves at the same temperature where the change in the NMR intensity occurs. We assume that activation/deactivation of rotational molecular motion of hydration water molecules occurs at the steps of the NMR intensity at higher and lower temperatures during heating and cooling, respectively. The rotational motion is probably the initial stage of the eutectic phase separation. Tris additive to NaCl solution causes thermal shifts of the small endothermic peak and in the related NMR intensity. These qualitative differences indicate interactions of Na^+ and Cl^- ions with the small organic molecule constituents.

Keywords: Freezing and melting of solutions; Eutectic transitions; Tris; NaCl; Heat-flux DSC; NMR

1. Introduction

Phase transitions at temperatures below freezing of water are important in the investigation of biological systems [1]. The investigated substances are usually aqueous solutions of proteins that also contain buffers and sodium chloride. The interactions of protein, buffer molecules and NaCl with water on a microscopic level have been investigated by proton NMR intensity measurements [2,3]. Liquid–solid transitions can be characterized by the analysis of thermal reactions detected by DSC [4–6]. Enthalpies of freezing and melting are distinct from the thermal energy associated with heat capacity. Heat capacities are usually known and enthalpies of transitions can be determined. Structural transformations of solutes occur over a longer temperature range and the enthalpy changes are slow. Freezing or melting is distributed over a temperature range due to the various water phases present in aqueous solution samples and the concentration changes of the dissolved substance during transition. Sharp enthalpy changes are observed at the melting point of the solvent. At cooling, the sample freezes from a supercooled state and this appears as a sharp transition.

The present work is the introductory step leading up to the quantitative determination of hydration level of proteins. We studied the NaCl and buffer solutions in order to be able to distinguish clearly the sources of measured effects. The behavior of the NaCl and buffer solutions without protein allows separating the effects connected with the hydration of NaCl, buffer and protein. We used an approach that consisted of DSC supplemented by NMR intensity measurement [7].

2. Experimental

The TA Instruments^{TM} heat-flux-type DSC 2920 cell was employed. One important parameter that should be taken into account when measuring phase changes using calorimetry is the heat-conducting path between the temperature sensor, the sample and the heater. A comprehensive analysis of this parameter

* Corresponding author.
E-mail address: kamasa@szfki.hu (P. Kamasa).

0040-6031/$ – see front matter © 2007 Elsevier B.V. All rights reserved.
doi:10.1016/j.tca.2007.08.001

in heat-flux calorimeters are described in [8–12] and cited references. Based on those results, we applied correction for sample temperature described in Appendix A.

The enthalpy changes were obtained from a differential signal [13], which is the temperature difference ΔT between reference and sample branches:

$$\Delta H = K \int_{t_1}^{t_2} \Delta T \, \mathrm{d}t \tag{1}$$

Once the calorimeter constant K is calibrated, the specific heat c_p of a sample of mass m can be determined from the measured ΔT at a given heating rate q, as follows:

$$mc_p = K\frac{\Delta T}{q} \tag{2}$$

The constant K was determined from the latent heat of ice–water transition ($\Delta H_{H_2O} = 333.8\,\mathrm{J\,g^{-1}}$ [14]) for double distilled water used for preparation samples, and measured under the same experimental conditions as sample mass and heating rate.

The enthalpy associated with heat capacity is minor in comparison to the enthalpies of phase transitions. For known heat capacities, enthalpies of transitions can be separated. In the case of an aqueous solution, the enthalpy of ice is subtracted from the total enthalpy of a partially melted solution.

The result normalized by latent heat of ice–water transition represents a water fraction in frozen solution:

$$\mathrm{fraction}(H_2O) = \frac{\Delta H_{\mathrm{solution}}(T) - \Delta H_{H_2O}(T)}{\Delta H_{H_2O}} \tag{3}$$

The number of water molecules associated with one formula unit of solute can be found as

$$\frac{n_{H_2O}}{n_{\mathrm{solute}}} = x\,\mathrm{fraction}(H_2O) \tag{4}$$

where x is the numerical ratio of the solvent molecules to the solute molecules in the completely melted state obtained from wt%:

$$x = \frac{M_{\mathrm{solute}}(100 - \mathrm{wt\%})}{\mathrm{wt\%}\, M_{H_2O}} \tag{5}$$

M_{solute} and M_{H_2O} are molecular masses of solute and water, respectively.

It is supposed implicitly that all the changes in the thermal quantities, e.g. in the specific heat and heat of melting are in direct correlation with the changes in mobility of water molecules. Heat associated with dilution of the crystalline salt in the just melt ice during solid–liquid transition was estimated to be negligibly small, below 2% of the heat of eutectic phase melting [15]. All DSC experiments were carried out on 20 μl of liquid that were heated and cooled at 2 K/min.

Details of the NMR method are given in [16]. In the present experiment, samples were cooled in nitrogen gas down to −70 °C and then heated at $5\,\mathrm{K\,min^{-1}}$ with measurements carried out at isothermal steps. The sample was determined to be at thermal equilibrium when the NMR signal intensity was stable for at least 5 min. To obtain the mobile water fraction, the intensity of the corresponding NMR-signal component was normalized to the signal intensity of liquid water measured above 0 °C.

2.1. Samples

Double distilled water was used as a reference substance to obtain calibration data and parameters for the temperature correction (see Appendix A). Sodium chloride solution was prepared by dissolving the appropriate quantity of NaCl(s) (Aldrich, 98+%) in double distilled water. The buffer solution was prepared from 150 mM NaCl, 50 mM Tris (Sigma) and 1 mM EDTA (Sigma) at pH 7.0 (Tris: tris(hydroxymethyl)-aminoethane; EDTA: ethylene diamine tetraacetic acid) dissolved in double distilled water.

For each solution composition, we carried out the NMR and DSC measurements on three to five samples prepared independently. The obtained data were reproducible within the 2% of maximum deviation.

3. Results

Thermal behavior recorded by DSC and NMR intensity for 9 wt% NaCl aqueous solution are depicted together in Fig. 1. The DSC data show two-phase transitions (Fig. 1, top panel). At cooling, rapid freezing of primary ice from supercooled liquid evolves enough heat to make not only a negative heat flow (exothermal) to appear but also to cause a visible increase of the sample temperature itself (point c_1). A second exothermal transition associated with freezing of the eutectic phase is observed at point c_2. This transition is less rapid with smaller differential signal. At heating, two endothermic peaks are observed in reverse order. First the eutectic melting is observed at T_e and then continuous melting of water with maximum at T_f.

The NMR measurement was carried out in the same temperature range during freezing and melting (Fig. 1, bottom panel). When the liquid is cooled below freezing, the sample remains

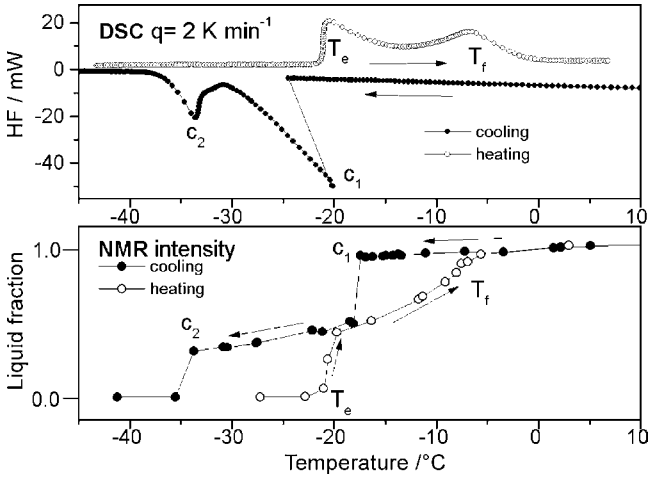

Fig. 1. Thermal response recorded in DSC experiment and evolution of the mobile water fraction obtained from NMR experiment during cooling and heating of 9 wt% NaCl aqueous solution.

supercooled until the point c_1, where the water spontaneously freezes. When the remaining unfrozen water phase is cooled further, the mobile water fraction slowly drops until a second transition at point c_2, where the signal intensity falls to zero. During heating cycle (open circles), no mobile water is detected until the temperature T_e is reached, where the mobility of water molecules increases rapidly to the value before freezing. From that point, the intensity rises smoothly until the temperature T_f, where only liquid is present.

Comparing DSC and NMR results, the same type of transitions can be easily distinguished. The temperatures of transitions at cooling may not be exactly the same due to supercooling. Freezing of primary ice was recorded in our DSC experiment at different temperatures between −14 and −18 °C.

All quantitative estimations of heat associated with fractional melting (enthalpy) were done at heating starting with a frozen sample at low temperature. We assume the enthalpy difference between the solid (completely frozen solution below −45 °C) and the liquid (above 0 °C) states are caused essentially by melting of ice. According to that assumption, the number of mobile water molecules in relation to the number of solute molecules was obtained from enthalpy of melting using Eq. (4). Series of DSC measurements were carried out at different NaCl concentration; we present here the results for three concentrations of $x = 370$, 33 and 18 (Fig. 2).

For 0.9 wt% NaCl solution (150 mM, $x = 370$) the number of unfrozen water molecules at eutectic phase melting (−21 °C), n_{H_2O}/n_{NaCl}, calculated from enthalpy data and from NMR intensity are estimated to be 10 ± 0.5 and 9.2 ± 0.5, respectively (Fig. 2, top). This value is also in agreement with the value of 10.7 corresponding to 23.3 wt% NaCl of eutectic concentration solution [17].

Similar results were obtained for melting of frozen solutions with higher solute concentrations (Fig. 2, middle and bottom), however, the lower DSC traces may originate from the fact that the normalization was based on the latent heat of melting of ice at 0 °C. The ice in the sample is melting at a wide range of temperature below 0 °C for which the latent heat of transition has a smaller value as a function of temperature. Melting temperature is independent of the concentration. There is a close agreement with the NMR results. The effect of supercooling is observed at cooling (Fig. 2, open symbols).

A different freezing behavior was observed for the Tris buffer solution at the same concentration of 150 mM NaCl (Fig. 3). While freezing of pure sodium chloride solution took place in two stages, freezing of the eutectic phase of buffer solution was not detected in this experiment (left panel, Fig. 3). At heating, the Tris solution exhibited similar behavior as the NaCl solution—two stages of melting were observed (right panel, Fig. 3). A small endothermic peak in the buffer was shifted to a lower temperature (−24.6 °C) and then a continuous increase of heat was recorded up to 0 °C as in the NaCl solution.

To determine the temperature, at which the eutectic phase of the buffer solution forms during cooling, the DSC experiment was repeated several times as follows. The samples were cooled to different temperatures below −38 °C and then the melting endotherm was recorded while heating (Fig. 4). Cooling to −38 °C and a little below had no effect on eutectic phase formation—no endothermic peak was observed at heating. After cooling to −39.2 °C, a slight endotherm was observed at around −24 °C. The traces of melting do not change with extent of cooling below −42 °C. That means that total freezing of eutectic phase takes place at around −42 °C in the buffer solution.

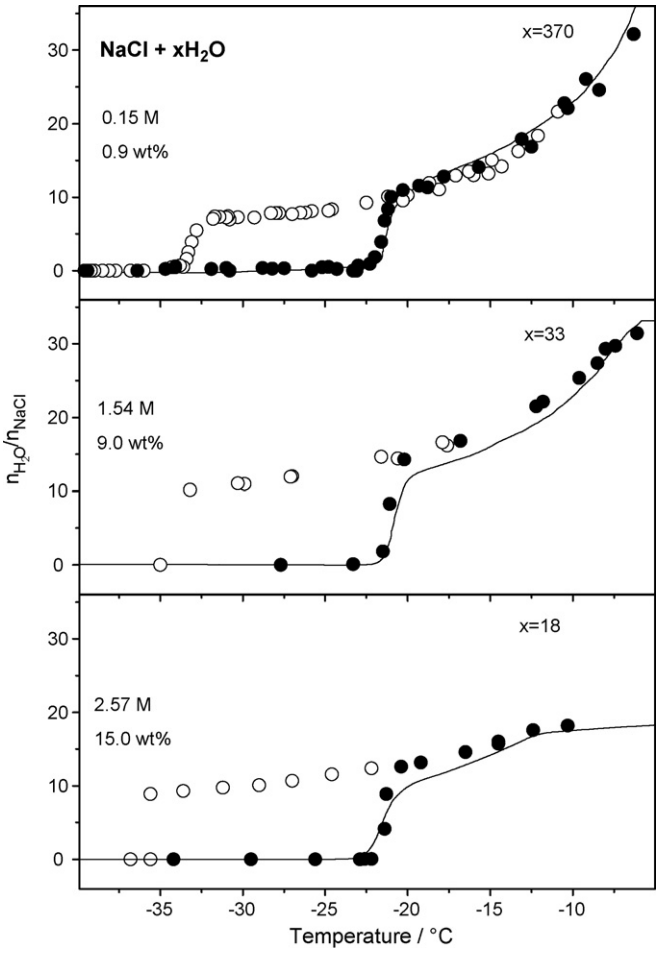

Fig. 2. Number of water molecules associated with one NaCl unit for different solution concentrations. Solid lines represent results from DSC experiment. The NMR results are depicted by symbols, at cooling—open and at heating—solid.

The NMR experimental results (Fig. 5) confirm the above conclusion. Part of the water rapidly freezes at point c_1 when supercooled by several degrees. The remaining mobile fraction is stable until the point c_2, where it decreases to zero. The temperature of -42 ± 0.5 °C of this transition is rather stable, as we have recorded during many experiments, in contrast to the supercooled NaCl solution with sharp freezing at higher temperatures (between −12 and −14 °C). The discrepancies between the results for NaCl and Tris stem from the fact that the NaCl–H_2O eutectic is a true binary eutectic. Such a system solidifies and melts at a single temperature while the eutectic observed in Tris sample is that of a "pseudo-binary" eutectic observed in multicomponent systems which changes phase in varying proportions over a finite temperature range.

Further analysis in the region of −20 to −45 °C indicates more complex transformations during heating for the buffer solution than for the NaCl solution as illustrated in Fig. 6. The

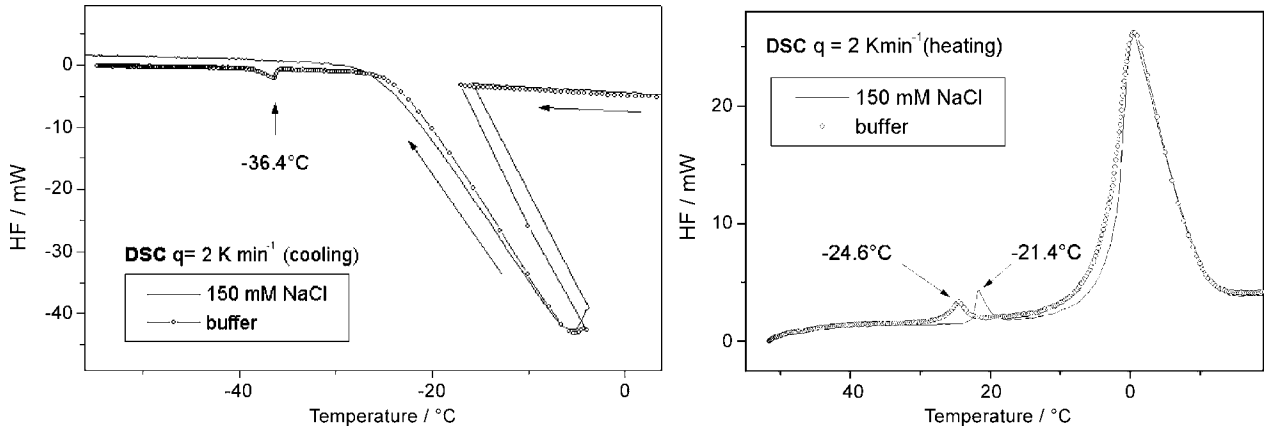

Fig. 3. DSC traces obtained during cooling (left) and heating (right) for 150 mM sodium chloride solution and for buffer solution.

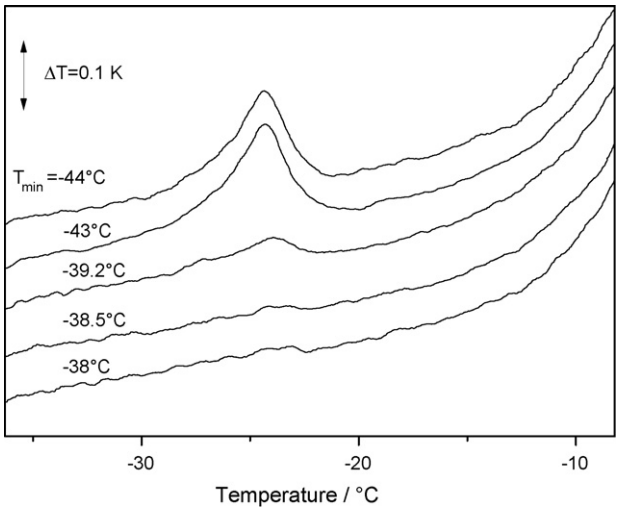

Fig. 4. The eutectic phase melting of buffer solution at heating recorded after cooling to different temperatures are indicated.

mobile water fraction in NaCl solution obtained by Eq. (3) is zero in both NMR (open triangles) and DSC (solid line) until the actual temperature reaches eutectic melting T_e(NaCl). On the other hand, the buffer solution exhibits similar transition of eutectic phase melting at T_e(buffer), which is preceded by the appearance of a small mobile fraction, beginning from temperature $T_H = -42\,^{\circ}C$. The growth of the mobile fraction by NMR intensity (open circles) has a step-wise character with plateau up to $-30\,^{\circ}C$ and then data follow at the same level with DSC. The initial growth obtained by DSC is smooth. This difference originates from the principles of two methods. The NMR intensity signal represents the number of protons as existing in a given phase, especially protons in a mobile state [3]. The normalized water fraction obtained from heat capacity is related to the microscopic motion of the molecules—linked to the total energy U of the microscopic system, which is temperature-dependent. This is the reason in numerical values of mobile water fraction at early stage of melting at $-42\,^{\circ}C$.

The comparison of curves made between the buffer and simple NaCl solutions depicted in Figs. 2–6, reveals qualitative differences between the two solutions. The most significant is that complete freezing of buffer solution takes place at $-42\,^{\circ}C$ as was found in experiment illustrated in Fig. 4. Freezing of NaCl solution took place at not lower temperature than $-37\,^{\circ}C$ in our experiment. Also at heating the partial melting for buffer solution is observed at $-42\,^{\circ}C$. The low and relatively constant temperature of freezing of buffer solution is a consequence of

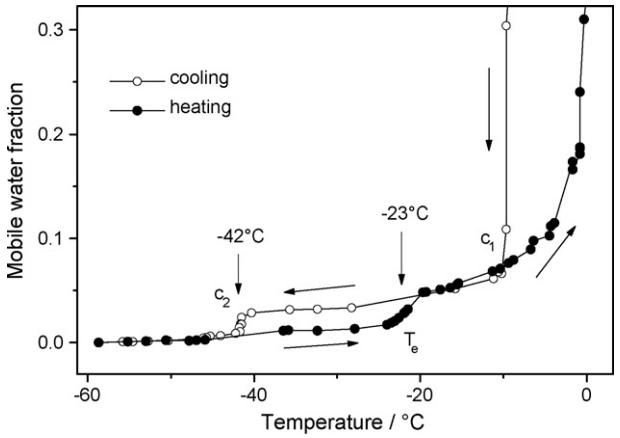

Fig. 5. Mobile water fraction obtained from NMR intensity signal for buffer solution during cooling and heating.

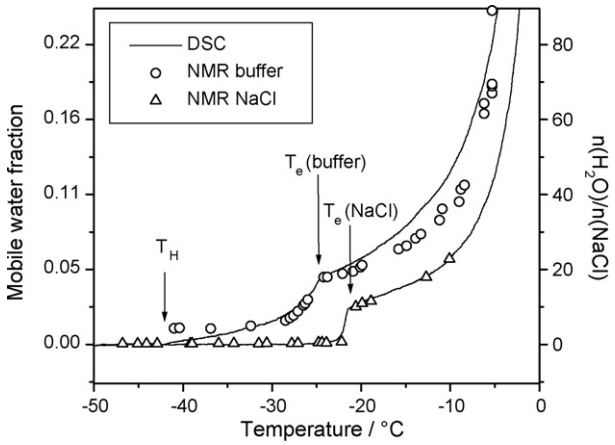

Fig. 6. Mobile water fraction obtained from DSC and NMR experiments for NaCl and buffer solutions during heating.

the hydration of the solute molecules Tris and EDTA as the NaCl concentrations are the same in the NaCl solution and in the buffer solution.

We think that Tris is a neutral agent from the chaotropic/kosmotropic point of view. Tris-buffer solution is used to wash out chaotropic agents from biological samples.

Described results point aspect of protein-independent hydration of solute ions abolished by the presence of the protein.

4. Conclusions

Several conclusions can build up from the above-described experimental results, concerning the low concentration solutions between inorganic and organic chemistry.

1. The DSC signal provides a macroscopic characterization through the heat capacity and the heat of transition, while the appropriate NMR signal intensity is directly proportional to the number of mobile water molecules and furnishes microscopic data. To analyze quantitatively effects recorded by these two methods, the integral value – the enthalpy – obtained from the heat flow, is qualitatively equivalent to the NMR signal intensity. The heat contributions not ascribable to the heat capacity of ice were interpreted as coming from mobile water molecules.
2. Steps of the NMR intensity have character of hysteresis loop versus temperature and are a result of activation/deactivation of rotational molecular motion of hydration water molecules at the appropriate temperatures. The rotational motion is probably the initial stage of the eutectic phase separation (the literary interpretation of thermal properties of salt solutions (brines) [18,19]). A small endothermic peak was detected in the DSC curves at the same temperature where the thermal hysteresis exists in the NMR intensity curves. For quantitative analysis, enthalpies of transitions were calculated from DSC data. There is good agreement for NaCl solutions, for all studied hypoeutectic concentrations.
3. The thermal behavior and the value of NMR intensities themselves are characteristically different for NaCl solution and Tris, that reveals the differences in the quantity and the kinetic behaviors of hydration shell water molecules. Tris and EDTA additives to NaCl solution cause thermal shifts of the small endothermic peak and in the related NMR intensity hysteresis. These qualitative differences indicate the interaction of Na^+ and Cl^- ions with the small organic molecule constituents.

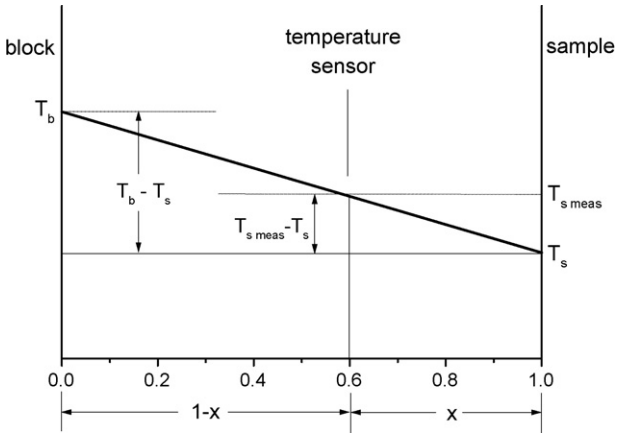

Fig. A.2. Sketch illustrating the temperature gradient through the path between block and sample. The value of $x = 0.4$ is characteristic to the TA2920 cell however it can differ even for the same type of calorimeter.

Acknowledgements

The work was partly supported by the International Senior Research Fellowship GR067595 from the Welcome Trust of Dr. Peter Tompa, thanks for him, and the authors also thank to Zoltán Pálmai undergraduate worker for his help in the measurements.

Appendix A. Sample temperature correction

The heat-conducting path from the temperature sensor to the sample depends on the construction of the calorimeter. The sketch in Fig. A.1(left) shows the principle of the construction of the DSC cell for the discussion of heat paths between sample and thermocouple and block.

The relation between measured temperature T_{smeas} and real sample temperature T_s can be found by considering an electrical model of the sample branch in the calorimeter cell illustrated in

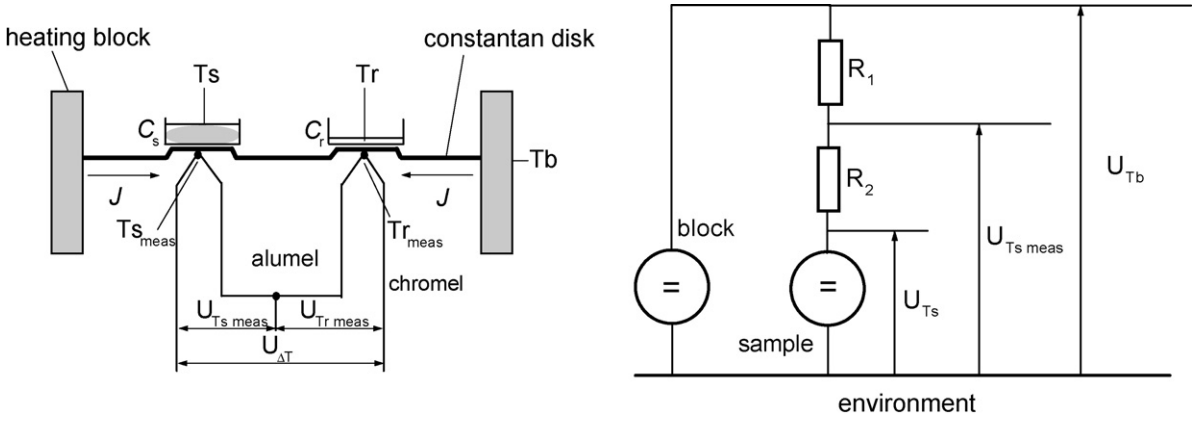

Fig. A.1. Schematic diagram of the heat-flux TA Instruments DSC (left) and of electrical circuit illustrating situation during melting (right).

Fig. A.2(right). There are two sources of heat with infinite heat capacity, which means they have a constant temperature independent of the heat flow rate from or to the sample. One of them is the block temperature T_b, maintained by the temperature program. The second one is the sample at the melting temperature, which does not change during transition from ice to liquid. Considering the circuit in the equilibrium state, the voltage $U_{T_{smeas}}$ measured as compared to the environment equals to:

$$U_{T_{smeas}} = (U_{T_b} - U_{T_s})\frac{R_2}{R_1 + R_2} + U_{T_s} \quad (A.1)$$

where R denotes thermal resistances, R_1 between block and thermocouple, and R_2 between the sample and the thermocouple.

Taking into account the above-mentioned analogy between voltage and temperature, the sample temperature can be found as

$$T_S = \frac{T_{smeas} - xT_b}{1 - x} \quad (A.2)$$

where x is the fraction of thermal resistance of the path between the sample and the thermocouple, R_2, with respect to thermal resistance between the sample and the block, $R_1 + R_2$:

$$x = \frac{R_2}{R_1 + R_2} \quad (A.3)$$

The effect of heat-conducting paths can be also analyzed graphically considering the temperature gradient along the block-sample thermal path as illustrated in Fig. A.2. The construction of the figure is based on three points: block temperature, T_b, measured temperature, T_{smeas}, and a sample temperature at melting, T_s. The formula for calculating the value of the sample temperature T_s is found from the similar triangles with its perpendicular sides: $T_b - T_s$, $x + 1 - x$ and $T_{smeas} - T_s$, x as Eq. (A.2). The value of x can be found by iteration Eq. (A2) till the sample temperature, T_s, will be approximately constant at melting.

References

[1] R. Cooke, I.D. Kuntz, Annu. Rev. Biophys. Bioeng. 3 (1974) 95–126.
[2] P. Racz, K. Tompa, I. Pocsik, Exp. Eye Res. 28 (1979) 129–135.
[3] K. Tompa, P. Bánki, M. Bokor, G. Lasanda, J. Vasáros, J. Alloy Comp. 350 (2003) 52–55.
[4] M. Pyda, J. Polym. Sci., Part B: Polym. Phys. 39 (2001) 3038–3054.
[5] M. Pyda, Macromolecules 35 (2002) 4009–4016.
[6] M. Pyda, in: D. Lorinczy (Ed.), The Nature of Biological Systems as Revealed by Thermal Methods, Kluwer Academic Publisher, Amsterdam, 2004, pp. 307–333.
[7] P. Tompa, P. Bánki, M. Bokor, P. Kamasa, D. Kovács, G. Lasanda, K. Tompa, Biophys. J. 91 (2006) 2243–2249.
[8] T. Ozawa, Bull. Chem. Soc. J. 39 (1966) 2071.
[9] G.W.H. Höhne, Thermochim. Acta 22 (2) (1978) 347–362.
[10] K.H. Schönborn, Thermochim. Acta 69 (1–2) (1983) 103–104.
[11] I. Moon, R. Androsch, B. Wunderlich, Thermochim. Acta 357–358 (2000) 285–291.
[12] R. Androsch, B. Wunderlich, Thermochim. Acta 369 (2001) 67–78.
[13] B. Wunderlich, Thermal Analysis, Academic Press Inc., New York, 1990, Chapter 4.
[14] P. Atkins, J. de Paula, Elements of Physical Chemistry, fourth edition, W.H. Freeman, Oxford University Press, 2005.
[15] R.H. Wood, R.A. Rooney, J.N. Braddock, J. Phys. Chem. 78 (1969) 1673–1678.
[16] M. Bokor, V. Csizmok, D. Kovacs, P. Banki, P. Friedrich, P. Tompa, K. Tompa, Biophys. J. 88 (2005) 2030–2037.
[17] O.B. Yatsenko, I.G. Chudotvortsev, Inorg. Mater. 38 (2002) 1079.
[18] T. Koop, A. Kapilashrami, L.T. Molina, M.J. Molina, J. Geophys. Res. 105 (2000) 26393–26402.
[19] H. Cho, P.B. Shepson, L.A. Barrie, J.P. Cowin, R. Zaveri, J. Phys. Chem. B 106 (2002) 11226–11232.